Arsenolite: a quasi-hydrostatic solid pressure-transmitting medium

Arsenolite: a quasi-hydrostatic solid pressure-transmitting medium

J A Sans[1], **F J Manjón**[1], **C Popescu**[2], **A Muñoz**[3], **P Rodríguez-Hernández**[3], **J L Jordá**[4] **and F Rey**[4]

[1] Instituto de Diseño para la Fabricación y Producción Automatizada, Universitat Politècnica de València, 46022 Valencia, Spain
[2] CELLS-ALBA Synchrotron Light Facility, 08290 Cerdanyola, Barcelona, Spain
[3] Departamento de Física, Instituto de Materiales y Nanotecnología, Universidad de La Laguna, 38205, La Laguna, Spain
[4] Instituto de Tecnología Química (UPV-CSIC), Universitat Politècnica de València-Consejo Superior de Investigaciones Científicas, 46022 Valencia, Spain

E-mail: juasant2@upv.es

CrossMark

Abstract

This study reports the experimental characterization of the hydrostatic properties of arsenolite (As_4O_6), a molecular solid which is one of the softest minerals in the absence of hydrogen bonding. The high compressibility of arsenolite and its stability up to 15 GPa have been proved by x-ray diffraction measurements, and the progressive loss of hydrostaticity with increasing pressure up to 20 GPa has been monitored by ruby photoluminescence. Arsenolite has been found to exhibit hydrostatic behavior up to 2.5 GPa and a quasi-hydrostatic behavior up to 10 GPa at room temperature. This result opens the way to explore other molecular solids as possible quasi-hydrostatic pressure-transmitting media. The validity of arsenolite as an insulating, stable, non-penetrating and quasi-hydrostatic medium is explored by the study of the x-ray diffraction of zeolite ITQ-29 at high pressure.

Keywords: arsenolite, high pressure, pressure transmitting medium

(Some figures may appear in colour only in the online journal)

1. Introduction

Pressure is a primary thermodynamic variable that allows the tuning of material properties in a large range. Therefore, high-pressure experiments are important tools which help us to understand the properties of matter both under ambient and extreme conditions. The application of pressure to materials induces a great reduction in interatomic distances, which intensifies interatomic interactions. Hence, it allows the study of material properties in a broader range than that created by changing temperature, its thermodynamic parameter counterpart. Besides, high-pressure techniques are also extensively used to synthesize compounds with different crystalline structures and properties without variation of their chemical stoichiometry and to synthesize new and unexpected compounds [1].

The diverse high-pressure devices, experimental techniques and materials with different properties make it difficult to find the optimal conditions to obtain reliable results. Amongst all these conditions, the choice of the medium which transmits the pressure from the instrument to the compressed sample is extremely important. In most cases, the only requirement for this medium is to be a hydrostatic pressure-transmitting medium (PTM) according to Pascal's principle; i.e. a compound that allows the homogeneous application of pressure to the sample without directional or shear stress in its structure. In fact, the loss of hydrostatic conditions leads to uniaxial distortions which affect the compressibility of the structure and could produce non-rigorous results, which could make difficult their comparison with purely hydrostatic theoretical predictions [2].

The choice of an optimal PTM is based on the pressure range, the technique employed, and the material studied in a particular case, but the ease to manipulate and the difficulty of the loading procedure should also be considered. In pressure

ranges above 10 GPa, the use of gas PTMs such as argon [3, 4], neon [3, 5] or helium [6, 7] is preferred to assure a wider hydrostatic range [8]. However, the lack of reactivity and the wide range of hydrostaticity of noble gases contrast with the difficulty to manipulate them and the specific equipment required for the loading procedure. In fact, the use of these gases is limited to diamond anvil cells (DACs) and is barely applied for transport properties, except in temperature-dependent measurements.

On the other hand, in pressure ranges below 10 GPa, liquid fluids such as silicone oil [9, 10], FC84-FC87 Fluorinert mixture [11], Daphne 7474 [12], (16:3:1) methanol–ethanol–water [4], or (4:1) methanol–ethanol mixture [4] are extensively used as PTMs due to their good hydrostatic behavior at low pressure and the ease of loading in a DAC. The transparency of these PTMs in the visible region makes them ideal for spectroscopic studies in the UV–visible range, x-ray diffraction and low-frequency Raman scattering measurements. However, they have Raman peaks at high frequencies and exhibit a very high infrared response (due to vibrational properties of their characteristic carbon–hydrogen, carbon–oxide and hydrogen–oxide bonds) [13]. Consequently, transparent solid PTMs, like KBr, although exhibiting a strong non-hydrostatic behavior above 6 GPa [14], are preferred for infrared measurements and Raman measurements in the high-frequency region.

Some types of materials and techniques require solid PTM for their study under compression. Regarding materials, the study of open-framework structures, such as zeolites, needs the use of solid PTM since fluids could penetrate into the different porous cavities of the structure yielding to unexpected results in their compressibility. Regarding techniques, transport measurements at high-pressure usually require the use of an insulating and non-magnetic solid PTM so that a good electrical insulation between the studied sample and the electric contacts with the gasket (and also from metallic anvils in the case of using a large volume press) is ensured. For that purpose, some insulating solid compounds like NaCl [15], hexagonal-BN [16], Na [17] and epoxy [18] are exploited. The main drawback of these solid PTMs is that they exhibit rather non-hydrostatic behavior at room temperature.

Arsenolite (As_2O_3 indeed As_4O_6) is the cubic polymorph of arsenic oxide (space group 227, *Fd-3m*, $Z = 16$), whose hardness is intermediate between that of talc ($Mg_3Si_4O_{11} \cdot H_2O$) and gypsum ($CaSO_4 \cdot 2H_2O$); these two minerals being the softest materials on the Moss scale. This compound is a molecular solid with an open framework structure composed of discrete As_4O_6 molecular units, exhibiting strong covalent interatomic As–O bonds, which are linked by weak van der Waals forces in order to form a 3D solid structure. In particular, the structure of the As_4O_6 molecular cage can be described by the overlap of four pseudo-tetrahedral units consisting of an As atom surrounded by three O ligands and a cationic lone electron pair (LEP) in such a way that they form a ball with all cation and anion LEPs pointing towards the external part of the cage. Unlike other arsenic oxide polymorphs, pseudo-tetrahedra in arsenolite are configured in closed-compact adamantane-type As_4O_6 molecular cages
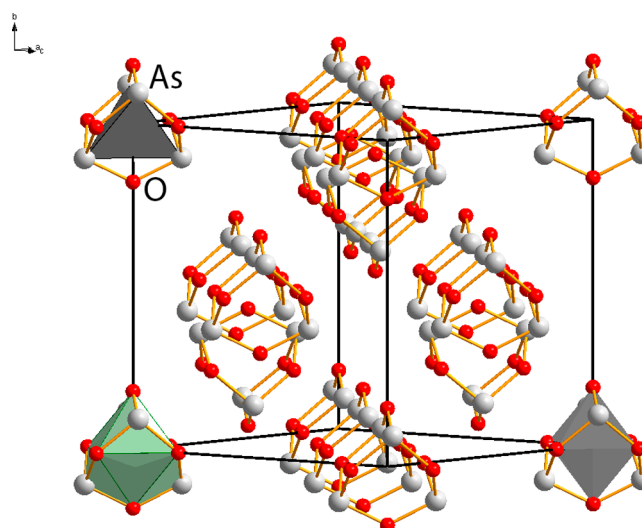

Figure 1. Detailed scheme of the unit cell of arsenolite (As_4O_6).

bonded together thanks to weak van der Waals forces (see figure 1). Among the properties of arsenolite, we can mention its strong chemical stability and lack of reactivity (it is an oxide mineral obtained by the oxidation of As-rich ore deposits as arsenic sulfide or by hydrolysis of arsenic chloride) [19] and that it is an insulating material with a band gap above 4 eV at room pressure and above 3 eV up to 15 GPa [20, 21]. In addition, the solubility of arsenolite has been fully characterized by a number of studies [22, 23] showing slow dynamics to reach the equilibrium conditions.

In this work, we will analyze the compressibility of arsenolite, its range of hydrostaticity, and how arsenolite can be applied to a case study, such as a zeolite, in order to show that arsenolite is an insulating solid compound, easy to manipulate, with a strong compressibility, high chemical inertness, and structural stability up to 15 GPa, which is a good candidate as a quasi-hydrostatic PTM up to 10 GPa in the measurements of structural and electrical properties under pressure. We will show that arsenolite is a better solid PTM than CsI, KBr, NaCl, and h-BN, so it could substitute for these solid PTMs in high-pressure experiments. The main drawback of arsenolite is its toxicity, but this could be easily overcome by handling it with gloves and mask, common equipment in high-pressure laboratories.

2. Method

Highly pure arsenolite (As_4O_6) powder (99.999%) has been commercially obtained from the Sigma Aldrich Company. Two high-pressure angle-dispersive x-ray diffraction (ADXRD) experiments at room temperature have been conducted in a membrane-type DAC. In the first experiment, we have studied the equation of state (EoS) of arsenolite [19] using as the PTM either a 4:1 methanol–ethanol mixture or silicone oil, but also without any PTM. The pressure inside the DAC was calibrated through the EoS of copper [24]. In the second, we have studied the structural evolution of zeolite ITQ-29 under compression using arsenolite as a PTM. In this latter experiment, the EoS of copper [24] and arsenolite [19] were used as

pressure callibrants. A good agreement has been obtained in the estimation of the pressure by both materials. Both ADXRD experiments have been performed at the BL04-MSPD beamline [25] of ALBA synchrotron with an incident monochromatic wavelength of 0.4246 Å focused to 20×20 μm with a pinhole of 50 μm to cut the x-ray beam tail. Images have been collected using a SX165 CCD detector. 1D diffraction profiles of intensity as a function of 2θ have been obtained by integration of the observed 2D diffraction patterns with the Fit2D software [26].

In addition, we have carried out two photoluminescence (PL) experiments. In the first, we have measured the PL of a 5 μm size ruby, which was placed into the center of the cavity pressure at room temperature using arsenolite as a PTM. In the second, we have measured the PL of four ruby chips of similar dimensions randomly distributed from the center to the edge of the pressure cavity. This last experiment has allowed us to determine the standard deviation of the pressure estimation along the cavity. Both PL measurements have been performed with a Horiba Jobin Yvon LabRAM HR-UV microspectrometer equipped with a thermoelectric-cooled multi-channel CCD detector and with a spectral resolution below $2\,cm^{-1}$. A HeNe laser (632.8 nm line) has been used to excite the ruby PL [27]. No detectable influence of the laser radiation on the temperature of the illuminated ruby chip has been found.

3. Results and discussions

In a previous work, we reported the structural characterization of compressed arsenolite by means of ADXRD measurements under compression using different PTMs [19]. It was reported that a similar EoS of arsenolite was obtained using non-penetrating PTMs, but a completely different result was obtained when He was used as a PTM due to its inclusion into the arsenolite's crystalline structure [19, 20]. In particular, non-penetrating PTM gave rise to a bulk modulus of $B_0 = 7(1)$ GPa, which is in good agreement (see figure 2) with our theoretical calculations [19] ($B_0 = 7.6$ GPa). It must be stressed that arsenolite's bulk modulus is much lower than those reported for a commonly used solid PTM, such as CsI [28] ($B_0 = 13.0$ GPa), KBr [29] ($B_0 = 14.4$ GPa), NaCl [30] ($B_0 = 25.03(8)$ GPa), and h-BN [31] ($B_0 = 29.1(4)$ GPa).

It is well known that hydrostatic conditions are closely determined not only by the bulk modulus, but by the shear modulus, which does not imply a volume change. Our theoretically simulated elastic properties of arsenolite [19] yield a shear modulus of 9.3 GPa under ambient conditions, which is in the order of that found in CsI (6.2–8.7 GPa) [28] and lower than the values reported for KBr [32] (14.8 GPa) and NaCl [33] (14.9 GPa). Unfortunately, we cannot give a value for the shear modulus of h-BN due to the lack of experimental measurements and the large discrepancy in theoretical values found in the literature, which was already exposed by Ooi and co-workers [34]. In spite of this lack of information on h-BN, we can suggest a value for the shear modulus of h-BN of around 15 GPa on the basis of the strong relationship between the bulk and shear moduli found in similar compounds.
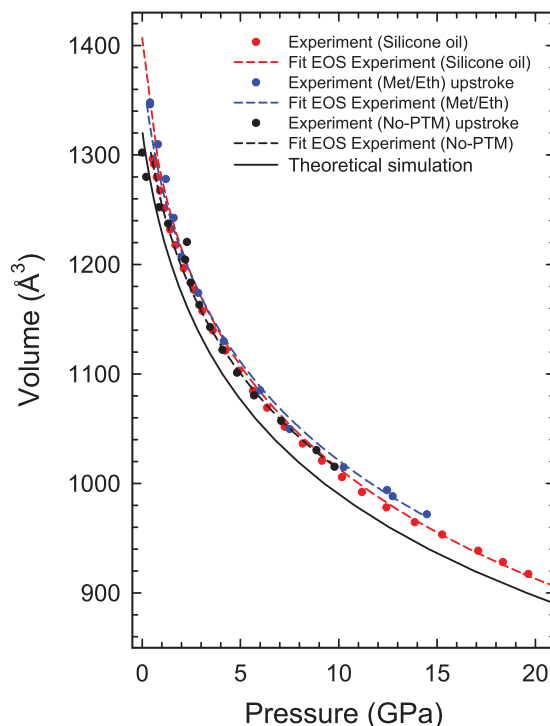

Figure 2. EoS of compressed arsenolite measured using an experimental ethanol–methanol mixture (blue points), silicone oil (red points) and without PTM (black points). EoS fit to a third-order Birch–Murnaghan equation is plotted with dashed lines and the evolution of the theoretically simulated structure of compressed arsenolite is plotted with a solid line.

The remarkably small bulk and shear moduli of arsenolite here reported are given by the extraordinary compressibility of the intermolecular distances between the As_4O_6 molecular cages (see figure 1). The presence of cation and anion LEPs is responsible for the formation of the molecular cages and the weak van der Waals interactions that bond them. Whereas these molecular units remain almost unalterable with increasing pressure due to the small reduction in intramolecular distances, the intermolecular distance between the different cages is rapidly reduced below 10 GPa due to the strong compressibility of the cationic LEP; i.e. the LEP activity progressively decreases with increasing pressure as observed in a number of group-15 related compounds [35]. The strong compression of intermolecular distances results in a strong increase in intermolecular interactions. These interactions are proposed to trigger the instability of molecular cages leading to a pressure-induced amorphization (PIA) of arsenolite as observed in previous studies [19, 36]. In particular, arsenolite compressed without any PTM gives rise to the appearance of PIA above 10 GPa.

In order to explore the hydrostatic regime of arsenolite under pressure, we have analyzed the stress caused in ruby chips randomly distributed along the gasketed pressure cavity and surrounded by As_4O_6 [37]. For that purpose, we have conducted PL measurements of the peaks R_1 and R_2 of ruby (Cr-doped Al_2O_3), which correspond to internal transitions of the Cr^{3+} ion in corundum aluminum oxide. In particular, R_1 and R_2 lines are assigned to transitions to the $^4A_2$ ground
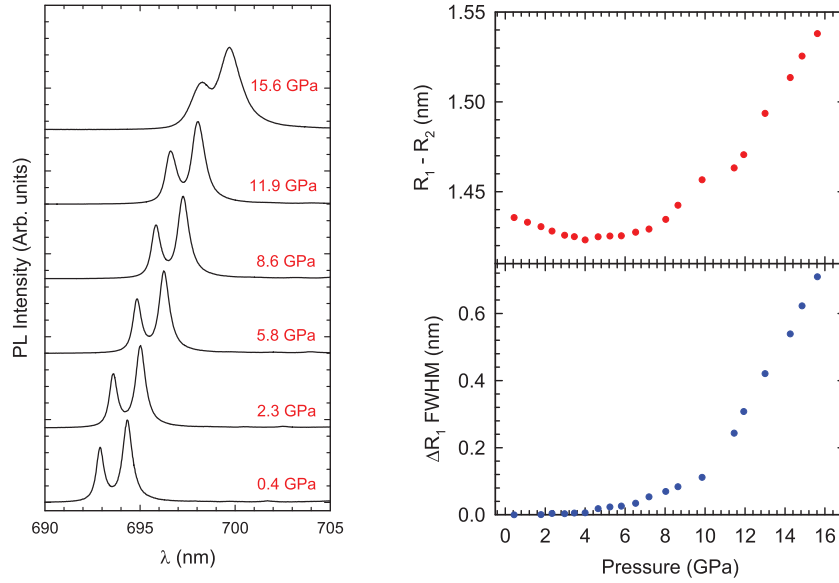
Figure 3. (a) PL spectra of R_1 and R_2 peaks of compressed ruby. They are vertically shifted for the sake of clarity. ((b): top) Evolution of the R_1–R_2 peak splitting with increasing pressure for a ruby chip surrounded by arsenolite inside a DAC and (((b): bottom)) idem for the FWHM of the R_1 peak.

state from the $2\overline{A}$ and $\overline{E}$ states (originated from the degeneracy break of the ^2E excited state), respectively [38–43]. The application of pressure causes an increase in the trigonal crystal-field strength, which induces a change in the transition energy of both lines [44]. Besides, the crystal-field strength depends strongly on directionality, which makes this parameter very sensitive to shear stress. The evolution of the R_1–R_2 splitting should remain nearly constant with pressure as long as hydrostatic conditions are satisfied, but the splitting increases once the pressure applied is not homogeneous.

The analysis of the R_1 and R_2 peaks serves to study the effect of the hydrostaticity in ruby [44]. However, the evolution of the full width at half maximum (FWHM) of both peaks under pressure can also be used as a method to determine the pressure gradients and local shear stresses [45]. Piermarini *et al* reported the broadening of the R_1 peak with the solidification of several liquid PTMs and suggested the distribution of several rubies along the pressure cavity in order to determine the standard deviation of the pressure calculated from each one, as the optimal method to accurately obtain the hydrostatic range of the medium [45]. Later, Klotz *et al* [8] used this method to determine the hydrostatic range of 11 PTMs. In most cases, both methods were found to be equivalent and gave rise to similar results. In fluid PTMs, the determination of the critical pressure at which the medium solidifies and loses the hydrostatic behavior strongly depends on the position of the ruby [8]. For this reason, the latter method is perfectly suited to the study of fluid PTMs, but it gives similar results to the former in the case of solid PTMs. Here, we report the hydrostatic range of arsenolite by both methods, analyzing the PL lines of a ruby chip under pressure and estimating the standard deviation of the pressure calculated from rubies randomly distributed along the pressure cavity.

For the first method, we inserted a ruby chip into the center of a pressure cavity. Figure 3 shows the peaks corresponding
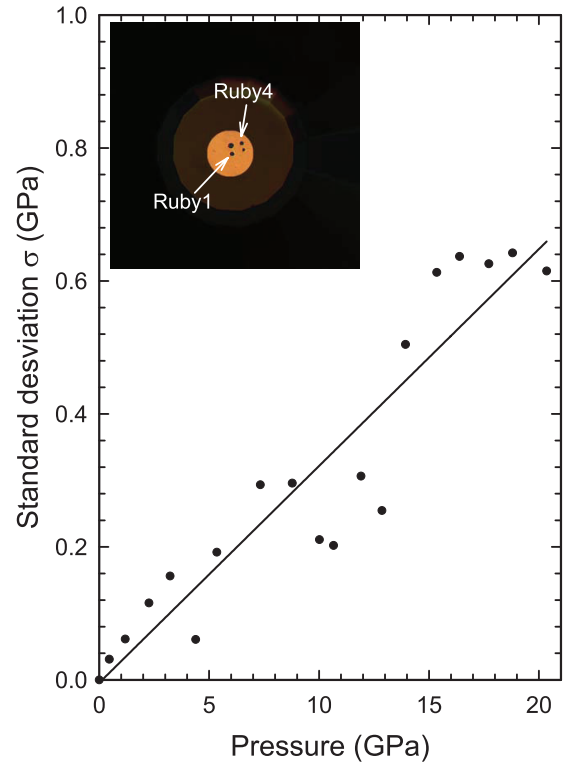

Figure 4. Pressure dependence of the standard deviation (σ) calculated using arsenolite as the PTM. Inset shows the distribution of ruby chips along the pressure cavity.

to the optical emission lines R_1 and R_2 of this ruby. A fit of these peaks to a Voigt-shape function (Lorentzian profile convoluted with a Gaussian function), which takes into account the resolution of the spectroscopic system given by the Gaussian convolution, allowed us to extract the amplitude, central wavelength, and FWHM of the Lorentzian peaks. The R_1–R_2 splitting shows a typical monotonous decrease up to
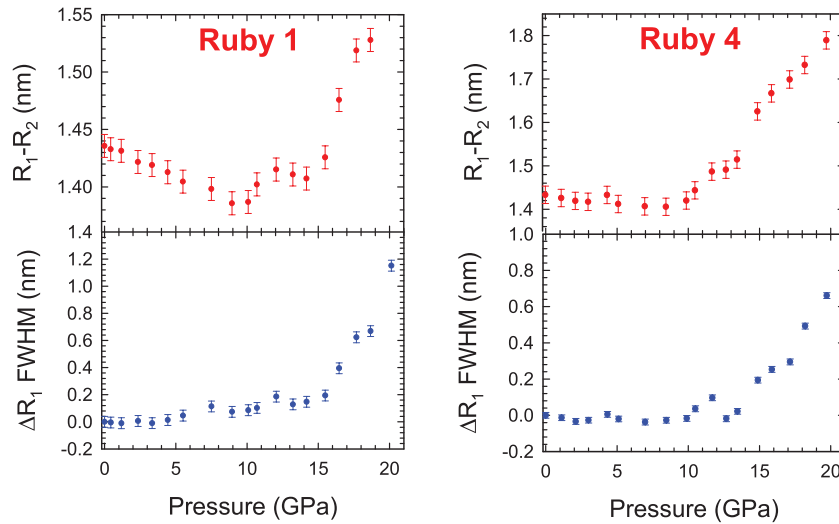
Figure 5. Evolution of the R_1–R_2 peak splitting and FWHM of the R_1 peak with increasing pressure for (a) ruby1 and (b) ruby4.

4–5 GPa, which is characteristic of hydrostatic behavior under pressure (figure 3(b) top). Above this pressure, we can observe a progressive non-linear increase in this parameter with pressure, which is more marked above 10 GPa. These features have been associated to the presence of deviatoric stresses in the ruby chip [44]. This result is confirmed by the increase in the FWHM (figure 3(b) down) of the R_1 peak above 4 GPa, this being more abrupt progressive broadening from 10 GPa.

Arsenolite's results can be compared with those of other solid PTMs. For instance, a progressive broadening of the R_1 peaks is observed at very low pressure in NaCl [46], so we can conclude that NaCl does not behave as a hydrostatic PTM even at ambient pressure. On the other hand, KBr shows deviatoric stresses in its structure when it transits from B_1 to B_2 phase above 2.1 GPa [14]. Moreover, the hydrostatic range here reported for arsenolite is better than some typical liquid PTMs such as Fluorinert mixture [8] (hydrostatic up to 2 GPa) and comparable to Daphne 7474 [8, 12] (hydrostatic up to 4 GPa), iso-n-pentane (hydrostatic up to 5–6 GPa) and silicone oil [8] (hydrostatic up to 4–8 GPa). However, its range of hydrostatic behavior is lower than that of methanol–ethanol mixtures [8] (hydrostatic up to 10.5 GPa for 16:3:1 methanol–ethanol–water and 4:1 methanol–ethanol mixture).

For the second method, we have randomly distributed four ruby chips from the center to the border of the gasketed pressure cavity, as shown in the inset of figure 4. The distance between the rubies is estimated from the size of the pressure cavity to be roughly 40 microns. This method shows that the hydrostatic range exhibited by arsenolite is very limited, since the standard deviation (figure 4) is less than 0.1 GPa below 2.5 GPa. This means that arsenolite exhibits a similar behavior to the mixture 1:1 FC84-FC87 Fluorinert, where the hydrostatic range extends to 2.3 GPa [8]. It is worth noting that the value of the standard deviation shows a small value in the high-pressure regime (~0.6 GPa at 20 GPa), which is competitive with those obtained in liquids. For instance, at 20 GPa, the standard deviation for different liquids is: ~2 GPa for 4:1 methanol–ethanol and 16:3:1 methanol–ethanol–water mixture and ~2.2 GPa for silicone oil. Figure 5 shows the analysis of the stress produced
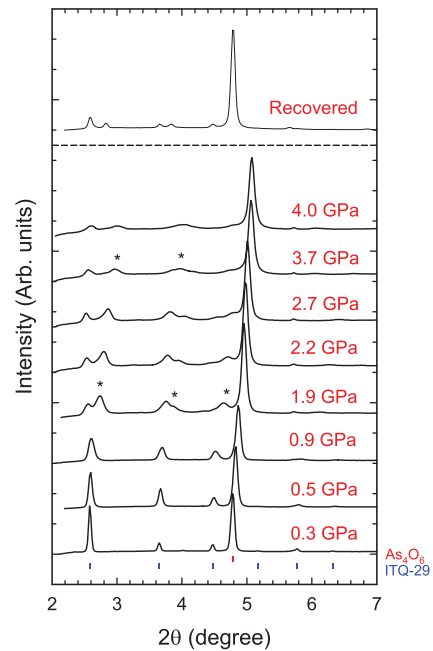

Figure 6. ADXRD patterns of ITQ-29 zeolite using arsenolite as the PTM inside a DAC. Asterisks indicate the new peaks appearing in the different transitions already reported. They are vertically shifted for the sake of clarity. The pattern of the recovered sample after pressure release shows the irreversibility of the second phase transition.

in the most centered and remote ruby (named ruby1 and ruby4, respectively), which reveals a similar behavior below 10 GPa. In both rubies, the R_1–R_2 peak distance decreases up to 10 GPa and then increases. However, this difference increases more rapidly for ruby4 than for ruby1, thus indicating that the latter is more stressed. The pressure dependence of the FWHM corresponding to the PL of the R_1 peak for both rubies yields similar results, as shown in figure 5. These findings corroborate the quasi-hydrostatic behavior observed in the standard deviation, with values smaller than 0.3 GPa up to 10 GPa.

Finally, the good properties of arsenolite as a PTM have been corroborated by analyzing the structural evolution of zeolite

ITQ-29 under compression [47]. This compound has an open framework structure with cavities of different sizes, so the use of fluid PTM, which might penetrate any of these cavities, must be avoided in high pressure studies. Besides, this compound is quite sensitive to non-hydrostatic conditions due to its molecular structure. Uniaxial distortions could easily induce structural deformations, which can be the onset of a phase transition. In this regard, the structural behavior of zeolite ITQ-29 with pressure was already reported using silicone oil as a PTM and two phase transitions were observed [48]. The cubic symmetry of arsenolite gives rise to few Bragg diffraction peaks, reducing the possibility of overlapping with the sample pattern. A fully reversible one at 1.2 GPa and a non-reversible one around 3.2 GPa, which leads to obtaining the novel zeolite ITQ-50 under ambient conditions. Figure 6 displays the evolution of the ADXRD patterns of zeolite ITQ-29 under compression using arsenolite as a PTM. As observed, our experiment shows a similar behavior to the one previously reported using silicone oil [48]. Between 0.9 and 1.9 GPa, there is a distortion of the cubic structure of ITQ-29, which is consistent with the transition pressure of 1.2 GPa already reported. Similarly, the irreversible phase transition is completed between 2.7 and 3.7 GPa in our experiment, which is consistent with the transition pressure of 3.2 GPa already reported. Therefore, the good agreement between the results obtained in this experiment and the previous one using silicon oil validate the use of arsenolite as a non-penetrating quasi-hydrostatic PTM.

4. Conclusions

We have shown that arsenolite, the cubic polymorph of arsenic oxide, is a solid insulating compound, easy to manipulate, with very low bulk and shear moduli, high chemical inertness, and structural stability up to 15 GPa, which shows a good hydrostatic range for a solid compound (up to 2.5 GPa) at room temperature. Therefore, we propose arsenolite as a good candidate for a quasi-hydrostatic PTM up to 10 GPa at room temperature in the measurement of electrical properties under pressure and for high-pressure structural studies of porous compounds and materials with open-framework structures in order to avoid penetration of the PTM inside their cavities. In addition, this work paves the way to explore other molecular solids as possible quasi-hydrostatic PTM.

Acknowledgments

References

[1] Hemley R J and Ashcroft N W 1998 *Phys. Today* **51** 26
[2] Mujica A, Rubio A, Muñoz A and Needs R J 2003 *Rev. Mod. Phys.* **75** 863
[3] Bell P M and Mao H K 1981 *Carnegie Institution of Washington Year Book* vol 80 (Washington, DC: Carnegie Institution of Washington) p 404
[4] Angel R J, Bujak M, Zhao J, Gatta G D and Jacobsen S D 2007 *J. Appl. Cryst.* **40** 26
[5] Meng Y, Weidner D J and Fei Y 1993 *Geophys. Res. Lett.* **20** 1147
[6] Takemura K and Dewaele A 2008 *Phys. Rev.* B **78** 104119
[7] Dewaele A and Loubeyre P 2007 *High Press. Res.* **27** 419
[8] Klotz S, Chervin J-C, Munsch P and Le Marchand G 2009 *J. Phys. D: Appl. Phys.* **42** 075413
[9] Ragan D D, Clark D R and Schiferl D 1996 *Rev. Sci. Instrum.* **67** 494
[10] Shen Y, Kumar R S, Pravia M and Nicol M F 2004 *Rev. Sci. Instrum.* **75** 4450
[11] Sidorov V A and Sadykov R A 2005 *J. Phys.: Condens. Matter* **17** S3005
[12] Murata K *et al* 2008 *Rev. Sci. Inst.* **79** 085101
[13] Howle C R, Homer C J, Hopkins R J and Reid J P 2007 *Phys. Chem. Chem. Phys.* **9** 5344
[14] Zhao J and Ross N L 2015 *J. Phys.: Condens. Matter* **27** 185402
[15] Meade C and Jeanloz R 1988 *J. Geophys. Res.* **93** 3270
[16] Piszora P, Nowicki W, Darul J and Lathe C 2010 *Synchrotron Radiat. Nat. Sci.* **9** 145
[17] Hanfland M, Syassen K and Köhler J 2002 *J. Appl. Phys.* **91** 4143
[18] Singh A K and Kennedy G C 1977 *J. Appl. Phys.* **48** 3362
[19] Brauer G (ed) 1963 *Handbook of Preparative Inorganic Chemistry* 2nd edn (New York: Academic)
[20] Sans J A *et al* 2016 *Phys. Rev.* B **93** 054102
[21] Gunka P A, Dziubek K F, Gładysiak A, Dranka M, Piechota J, Hanfland M, Katrusiak A and Zachara J 2015 *Cryst. Growth Des.* **15** 374
[22] Pokrovski G S, Bény J-M and Zotov A V 1999 *J. Solut. Chem.* **28** 1307
[23] Nordstrom D K, Majzlan J and Königsberger E 2014 *Rev. Min. Geochem.* **79** 217
[24] Dewaele A, Loubeyre P and Mezouar M 2004 *Phys. Rev.* B **70** 094112
[25] Fauth F, Peral I, Popescu C and Knapp M 2013 *Powder Diffr.* **28** S360
[26] Hammersley A P, Svensson S O, Hanfland M, Fitch A N and Hausermann D 1996 *High Press. Res.* **14** 235
[27] Garcia-Domene B *et al* 2012 *J. Appl. Phys.* **112** 123511
[28] Ribeiro R M, Coutinho J, Torres V J B, Jones R, Sque S J, Öberg S, Shaw M J and Briddon P R 2006 *Ab initio* study of CsI and its surface *Phys. Rev.* B **74** 035430
[29] Roberts R W and Smith C S 1970 *J. Phys. Chem. Solids* **31** 619
[30] Decker D L 1971 *J. Appl. Phys.* **42** 3239
[31] Fuchizaki K, Nakamichi T, Saitoh H and Katayama Y 2008 *Solid State Commun.* **148** 390
[32] Matsokin V P and Petchenko G A 2000 *Low Temp. Phys.* **26** 517
[33] Gleason A E 2010 Elasticity of materials at high pressure *PhD thesis* Earth & Planetary Science, UC Berkeley
[34] Ooi N, Rajan V, Gottlieb J, Catherine Y and Adams J B 2006 *Modelling Simul. Mater. Sci. Eng.* **14** 515
[35] Pereira A L J, Sans J A, Vilaplana R, Gomis O, Manjón F J, Rodríguez-Hernández P, Muñoz A, Popescu C and Beltrán A 2014 *J. Phys. Chem.* C **118** 23189
[36] Grzechnik A 1999 *J. Sol. State Chem.* **144** 416

[37] Chervin J C, Canny B and Mancinelli M 2001 *High Press. Res.* **21** 305

[38] Sugano S and Tanabe Y 1958 *J. Phys. Soc. Japan* **13** 880

[39] Sugano S and Tsujikawa I 1958 *J. Phys. Soc. Japan* **13** 899

[40] Schawlow A L, Wood D L and Clogston A M 1959 *Phys. Rev. Lett.* **3** 271

[41] McClure D S 1959 Electronic spectra of molecules and ions in crystals part II, spectra of ions in crystals *Solid State Physics* vol 9, ed F Seitz and D Turnbull (New York: Academic) pp 399–524

[42] Ford R A 1960 *Spectrochim. Acta* **16** 582

[43] Low W 1960 *J. Chem. Phys.* **33** 1162

[44] Syassen K 2008 *High Press. Res.* **28** 75

[45] Piermarini G J, Block S and Barnett J D 1973 *J. Appl. Phys.* **44** 5377

[46] Tateiwa N and Haga Y 2009 *Rev. Sci. Inst.* **80** 123901

[47] Corma A, Rey F, Rius J, Sabater M J and Valencia S 2004 *Nature* **431** 287

[48] Jordá J L *et al* 2013 *Angew. Chem. Int. Ed.* **52** 10458